

# Twisting integrin receptors increases endothelin-1 gene expression in endothelial cells

JIANXIN CHEN,<sup>1</sup> BEN FABRY,<sup>1</sup> ERNESTO L. SCHIFFRIN,<sup>2</sup> AND NING WANG<sup>1</sup>

<sup>1</sup>Physiology Program, Department of Environmental Health, Harvard School of Public Health, Boston, Massachusetts 02115; and <sup>2</sup>Medical Research Council Multidisciplinary Research Group on Hypertension, Clinical Research Institute of Montreal, University of Montreal, Montreal, Quebec, Canada H2W 1R7

Received 26 April 2000; accepted in final form 19 January 2001

**Chen, Jianxin, Ben Fabry, Ernesto L. Schiffrin, and Ning Wang.** Twisting integrin receptors increases endothelin-1 gene expression in endothelial cells. *Am J Physiol Cell Physiol* 280: C1475–C1484, 2001.—A magnetic twisting stimulator was developed based on the previously published technique of magnetic twisting cytometry. Using ligand-coated ferromagnetic microbeads, this device can apply mechanical stresses with varying amplitudes, duration, frequencies, and waveforms to specific cell surface receptors. Biochemical and biological responses of the cells to the mechanical stimulation can be assayed. Twisting integrin receptors with RGD (Arg-Gly-Asp)-containing peptide-coated beads increased endothelin-1 (ET-1) gene expression by >100%. In contrast, twisting scavenger receptors with acetylated low-density lipoprotein-coated beads or twisting HLA antigen with anti-HLA antibody-coated beads did not lead to alterations in ET-1 gene expression. In situ hybridization showed that the increase in ET-1 mRNA was localized in the cells that were stressed with the RGD-coated beads. Blocking stretch-activated ion channels with gadolinium, chelating Ca<sup>2+</sup> with EGTA, or inhibiting tyrosine phosphorylation with genistein abolished twist-induced ET-1 mRNA elevation. Abolishing cytoskeletal tension with an inhibitor of the myosin ATPase, with an inhibitor of myosin light chain kinase, or with an actin microfilament disrupter blocked twisted-induced increases in ET-1 expression. Our results are consistent with the hypothesis that the molecular structural linkage of integrin-cytoskeleton is an important pathway for stress-induced ET-1 gene expression.

mechanical stress; cytoskeleton; prestress; mechanotransduction; magnetic twisting stimulator

---

ALTHOUGH IT IS KNOWN that mechanical forces are important in regulating many cell functions, such as cell growth, proliferation, protein synthesis, and gene expression (4, 8, 20), it is not well understood how mechanical signals are transduced into biological responses. Several methods have been developed to apply mechanical stresses and/or strains to cell surfaces of a single cell [micropipette aspiration (11, 16), cell poking (34), laser tweezers (6), and atomic force microscopy (43)] or to surfaces of a population of cells [flexible culture substrates (45) and fluid shear stresses (9, 22)].

The advantage of probing a single cell is that one could examine regional differences in mechanical properties of a single cell. The limiting factors are the significant variability among individual cells and a sample size that is too small to allow quantitation of protein synthesis or gene expression. The method of stretchable membrane or fluid shear flow has revealed valuable insights on how cells respond to mechanical perturbations but is limited at elucidating the initial specific mechanotransduction pathway.

We have developed a magnetic twisting cytometry (MTC) technique in which controlled mechanical stresses are applied directly to specific cell surface receptors via ligand-coated ferromagnetic microbeads, and cellular mechanical responses are measured simultaneously (49). Our previous studies revealed that external mechanical forces are transmitted across the cell surface and to the cytoskeleton via transmembrane cell adhesion molecules such as integrins (48–51), E-selectins (54), and E-cadherins (36), and, surprisingly, a glycosyl phosphatidylinositol-linked receptor, the urokinase receptor (52). We also quantitated receptor-specific cell mechanical properties in many different cell types, such as endothelial cells, airway smooth muscle cells, epithelial cells, cardiac muscle cells, and vascular smooth muscle cells (18, 21, 36, 46, 49–51). However, MTC is inherently limited by the small number of cells it can probe (typically about 30,000 cells/well), so it is difficult to assay gene expression and protein synthesis. In addition, MTC was not designed to hold more than one cell culture dish at a time, to apply mechanical stresses for long periods of time, or to alter the force waveform.

To circumvent these shortcomings of MTC, we developed a magnetic twisting stimulator (MTS) that can apply controlled mechanical twisting stresses with varying amplitudes, frequencies, and waveforms via specific receptors to a large number of cells in multiple cell culture dishes simultaneously.

Using our MTS, we examined the alterations of endothelin-1 (ET-1) gene expression in response to me-

---

Address for reprint requests and other correspondence: N. Wang, Physiology Program, Harvard School of Public Health, 665 Huntington Ave., Boston, MA 02115 (E-mail: nwang@hsph.harvard.edu).

---

The costs of publication of this article were defrayed in part by the payment of page charges. The article must therefore be hereby marked "advertisement" in accordance with 18 U.S.C. Section 1734 solely to indicate this fact.

chanical stresses applied via RGD (Arg-Gly-Asp)-coated ferromagnetic microbeads. ET-1 has been demonstrated to be a potent vasoconstrictor (55). ET-1 mRNA expression was found to be more than doubled after human umbilical vein endothelial cells (HUVECs) were subjected to cyclic strains (47). In contrast, ET-1 mRNA increases in response to low levels of fluid shear stress ( $<5$  dyn/cm<sup>2</sup>) (30) and high levels of fluid shear stress ( $>20$  dyn/cm<sup>2</sup>) applied for up to 2 h, but then decreases for longer durations (24, 25, 27, 42). It is still not clear what molecules mediate mechanical stress transmission and transduction when cells are stretched or sheared with fluid flow. We hypothesize that application of mechanical stresses via specific integrin receptors alters ET-1 mRNA expression. We also hypothesize that preexisting tension (prestress) in the cytoskeleton (CSK) is an important regulator of ET-1 gene expression in response to mechanical stress. In this study, we found that twisting magnetic beads bound to integrin receptors resulted in an increase in ET-1 mRNA expression. Furthermore, inhibiting the prestress in the CSK abolished elevation in ET-1 gene expression. Blocking stretch-activated ion channels, inhibiting tyrosine phosphorylation, or disrupting actin CSK all led to abolishing ET-1 gene expression elevation in response to stress applied to integrin receptors.

#### MATERIALS AND METHODS

**Reagents.** Fetal bovine serum (FBS), bovine serum albumin (BSA), heparin, trypsin-EDTA (500 U/ml trypsin and 180 µg/ml EDTA), phosphate-buffered saline (PBS) for cell culture, 1-ethyl-3-(3'-dimethylaminopropyl)carbodiimide, agarose, formaldehyde, ethidium bromide, MOPS-EDTA-sodium-acetate buffer, RNA sample loading buffer, sodium chloride, citric acid, and trisodium salt were obtained from Sigma Chemical (St. Louis, MO). Medium 199 and L-glutamine were purchased from GIBCO (Gaithersburg, MD). Penicillin, streptomycin, and fungizone were obtained from Bio Whittaker (Walkersville, MD). Endothelial cell growth supplement (ECGS) was purchased from Becton Dickinson Labware (Bedford, MA). Culture dishes (60 mm), gel blot paper, and autoradiography films were acquired from VWR (Philadelphia, PA). Acetylated low-density lipoprotein (AcLDL) was purchased from Biomedical Technologies (Stoughton, MA). RGD peptides were from Integra LifeSciences (San Diego, CA). Anti-histocompatibility leukocyte antigen (HLA) antibody was a gift from Dr. M. Chicurel. Ferromagnetic beads (4.5 µm in diameter) were from Spherotech (Libertyville, IL). Glacial acetic acid was obtained from Fisher (Pittsburgh, PA). Total RNA extraction kit, QIA shredders for homogenization, and gel extraction kit were obtained from Qiagen (Santa Clarita, CA). Quick spin columns for labeled nucleic acid purification were purchased from Boehringer Mannheim (Indianapolis, IN). Quick hybridization solution and random primer labeling kit were obtained from Stratagene (La Jolla, CA).

**Cell culture.** HUVEC cells were obtained from Clonetics (San Diego, CA) and cultured in medium 199, 20% FBS, 100 U/ml penicillin, 100 µg/ml streptomycin, 0.25 µg/ml fungizone, 60 µg/ml ECGS, and 50 µg/ml heparin at 37°C in a humidified atmosphere containing 5% CO<sub>2</sub>. For all experiments, cells were used between passages 5 and 10. The cells were plated in 60-mm dishes and grown to confluence in culture medium. Before addition of microbeads, the dishes

were washed twice with serum-free defined medium containing 1% BSA. Two milligrams of ligand-coated beads were added into each dish for 30 min in serum-free defined medium (average 10 beads/cell). Unbound beads were then gently washed off with serum-free defined medium.

**Coating of beads.** RGD and AcLDL were coated onto the beads at 50 µg of protein/mg of beads using the manufacturer's protocols (49, 51). Anti-HLA antibody was coated at 20 µg of protein/mg of beads as previously described (49, 54). Under these conditions, the coating densities resulted in maximum absorption of proteins onto the surface of the beads.

**Electron microscopy.** We used scanning electron microscopy (Amray 100A) to evaluate internalization of beads by the cells. After RGD-coated beads were added for ~1 h, the cells were fixed with 2% glutaraldehyde, dehydrated through a graded ethanol series, immersed in mixtures of ethanol and hexamethyldisilazane (HMDS; Electron Microscopy Sciences) with 33, 66, and 100% HMDS for 15 min, and air-dried. The bottom of the cell well was cut off with a hot tungsten wire, and the cells were sputtered with gold palladium. The HUVECs internalized  $>70%$  of the beads when beads were added at ~10 beads/cell.

**Immunofluorescence.** The cells were grown in Lab-Tek eight-well culture slides (Nalge Nunc International) until confluence. RGD-coated beads were added to the wells for 8 h. Some cell wells were then treated with 0.1 µg/ml of cytochalasin D (Cyto D) for 30 min. The cells were fixed in 2% paraformaldehyde in room temperature and washed twice with PBS. The cells were then treated with 0.2% Triton X-100 and 0.1% BSA in PBS for 15 min. Rhodamine-phalloidin (200 nM; Cytoskeleton, Denver, CO) was added and kept overnight. The wells were washed three times with PBS before Prolong antifade kit mounting solution (Molecular Probes, OR) was added to the center of each well and a coverslip was mounted and sealed on top of the slide. The wells were stored in the dark at 4°C before being viewed with a laser confocal microscope (TCS NT; Leica).

**RNA isolation and Northern analysis.** After mechanical stimulation of the cells, the supernatant was collected and the cells were lysed in guanidinium isothiocyanate (GITC)-containing buffer. Total cellular RNA was obtained after homogenization and extraction. RNA concentration and relative purity were quantified by measuring absorbance at 260 nm and the ratio of the absorbance at 260–280 nm. Ten milligrams of RNA were loaded per lane and separated on 1.3% agarose gel. After electrophoresis, RNA was transferred onto a nitrocellulose membrane by capillary blotting, immobilized by ultraviolet irradiation, and dried at 70°C for 2 h. The membrane was prehybridized for 30 min in Quick hybridization solution. Hybridization was then carried out in the solution containing <sup>32</sup>P-labeled cDNA specific for human ET-1 (gift of Dr. Arthur Lee) and for human glyceraldehyde-3-phosphate dehydrogenase (GAPDH; gift of Dr. Joe Paulauskis). After 3 h of incubation, the membrane was washed with 2× saline sodium citrate (SSC)-0.1% sodium dodecyl sulfate (SDS) at room temperature once, washed with 0.2× SSC-0.1% SDS at 55°C twice, and was then exposed to X-ray film at -80°C (24). The autoradiogram was scanned, and densitometry was carried out. The ratio of ET-1 to GAPDH densities was compared between groups.

**In situ hybridization.** A 1.2-kb EcoRI fragment of a cloned ET-1 cDNA (no. 65698; American Type Culture Collection, Rockville, MD) corresponding to part of the second exon of the human preproET-1 gene was subcloned into pGEM7zf<sup>+</sup>, as previously described (40). From this construction, the sense and antisense human cRNA probes were prepared by

RNA transcription reaction using T7 or SP6 RNA polymerase, respectively. Digoxin-labeled riboprobes were prepared with the DIG RNA labeling kit (Roche Molecular Biochemicals) according to specifications of the manufacturer.

After the twisting experiments, the cells on the slides were fixed with 4% paraformaldehyde. The slides were then treated with 0.3% Triton X-100 in PBS for 15 min and washed in PBS for 5 min. Deproteination was carried out with 50  $\mu\text{g}/\text{ml}$  of proteinase K (Roche Molecular Biochemicals) for 30 min at 37°C. Slides were washed with PBS, washed twice for 5 min, postfixed for 5 min with 4% paraformaldehyde, and washed again with PBS. Slides were transferred to 0.1 mol/l of triethanolamine, pH 8.0, and acetylated with 0.25% acetic anhydride (vol/vol) for 10 min. Slides were then rinsed in PBS and 100  $\mu\text{l}$  of fresh prehybridization solution (50% deionized formamide + 4 $\times$  SSC, pH 7.0) applied to each slide, followed by incubation in a humid chamber for 1 h. Sense and antisense strand digoxin-labeled human preproET-1 cRNA probes (20–100 ng/ml), previously denatured for 5 min at 65°C, were diluted in hybridization buffer (50% formamide, 0.5 mg/ml dextran sulfate, 4 $\times$  SSC, 1 $\times$  Denhardt's solution, 0.25 mg/ml yeast tRNA, and 0.5 mg/ml denatured salmon sperm DNA). After a brief wash with 2 $\times$  SSC, 50  $\mu\text{l}$  of hybridization solution with the probe were applied to each section, which were then covered with an autoclaved coverslip. Sections were incubated in the hybridization oven at 46°C overnight. The next day, the slides were washed in 2 $\times$  SSC. Slides were treated with RNase A (10  $\mu\text{g}/\text{ml}$ ) at 37°C for 30 min to remove single-strand RNA molecules. Successive washes at room temperature followed in 1 $\times$  and 0.1 $\times$  SSC for 15 min each. Detection of digoxin-labeled probes was performed with a Roche Molecular Biochemicals kit according to specifications of the manufacturer. Slides were incubated for 2 h at room temperature with alkaline phosphatase-conjugated anti-digoxin antibodies, washed with the detection buffer for 10 min, and then incubated overnight with 2-(4-iodophenyl)-5-(4-nitrophenyl)-3-phenyltetrazolium chloride/5-bromo-4-chloro-3-indolyl phosphate-*p*-toluidine salt (Boehringer). Specificity of labeling was established by incubating slides with the sense strand human preproET-1 cRNA probe.

**MTS.** To carry out the proposed studies, we built a prototype of an MTS. This device could apply mechanical stresses to multiple cell wells simultaneously via specific receptors. Figure 1 shows the schematic of the MTS. Spherical ferromagnetic beads that were coated with specific receptor ligands were allowed to bind to the surface of the cultured cells for 6 h. Brief application of a strong magnetic field (the magnetization field generated by Helmholtz coils) magnetized and aligned the magnetic moments of all beads in the horizontal direction. The two Helmholtz coils had a radius of 15 cm, each with 20 turns, separated by 15 cm. A cardiac

defibrillator (HP7802D) was connected to the Helmholtz coils to generate a short magnetic pulse with an intensity high enough to magnetize the ferromagnetic microbeads. The energy released during discharge was set at 300 J. To block any reverse current from the coils back to the capacitor, a high-voltage, high-current diode was connected between the capacitor and the Helmholtz coils. By applying a weaker magnetic field (twisting field generated by a solenoid) in the vertical direction, the beads were twisted in the direction of the twisting field and thereby exerted a rotational shear stress on those cell surface receptors that were bound to the beads. The maximum magnetic flux density (at a maximum charge of 400 J) is  $\sim 1,500$  gauss with a pulse duration of  $\sim 1$  ms. The solenoid had the following dimensions: diameter = 11 cm; length = 9 cm; number of turns = 400; wire gauge = 22 (0.644 mm); and resistance = 5  $\Omega$ . A current of 1 A produced a magnetic field of 35 gauss in the center of the coil. We measured the magnetic field within the twisting coil with a pickup coil attached to an oscilloscope while the current source generated a sinusoidal current of 100 Hz with an amplitude of 1 A. The magnetic field within the twisting coil decreased axially and increased radially, but variability remained within 9% over a volume equivalent to six 60-mm dishes stacked together. The beads from Spherotech generated a specific torque of 0.5  $\text{dyn}\cdot\text{cm}^2\cdot\text{gauss}^{-1}$  when the twisting field was oriented orthogonal to the remanent field vector. When the beads were internalized by the cells, they generated an apparent stress of 0.5  $\text{dyn}\cdot\text{cm}^2\cdot\text{gauss}^{-1}$  twisting field. To generate the waveform of the twisting current, and to program magnetization of the beads, a microcontroller (BS2-IC; Parallax) was used. The microcontroller generated a pulse-width modulated signal (8-bit resolution) that was low-pass filtered and converted into a current. The maximum current that could be generated by the device is 2.5 A, resulting in a maximum twisting field of 87.5 gauss (an apparent stress of 43.75  $\text{dyn}/\text{cm}^2$  for these beads). In this study, we applied constant twisting fields at 40 gauss (equivalent to 20  $\text{dyn}/\text{cm}^2$ ). Because the torque applied to the beads decreased as the function of cosine of the bead rotation angle (51), the beads were remagnetized every 10 min to reset the applied stress back to 20  $\text{dyn}/\text{cm}^2$ . The twisting coil was cooled by placing a coiled rubber tubing inside the solenoid coil that received circulating water from a water bath with adjustable temperature. Six 60-mm dishes with cultured cells were placed inside the twisting coil. The whole apparatus was placed inside an incubator during experiments for control of temperature and  $\text{CO}_2$ .

## RESULTS

After the RGD-coated beads were added for  $\sim 1$  h, most of the beads were already internalized, as re-

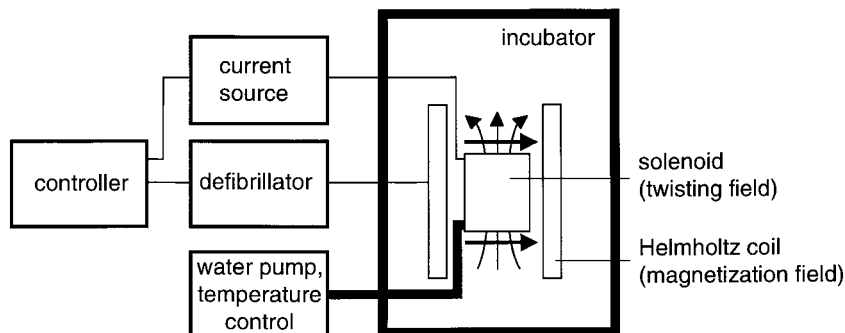
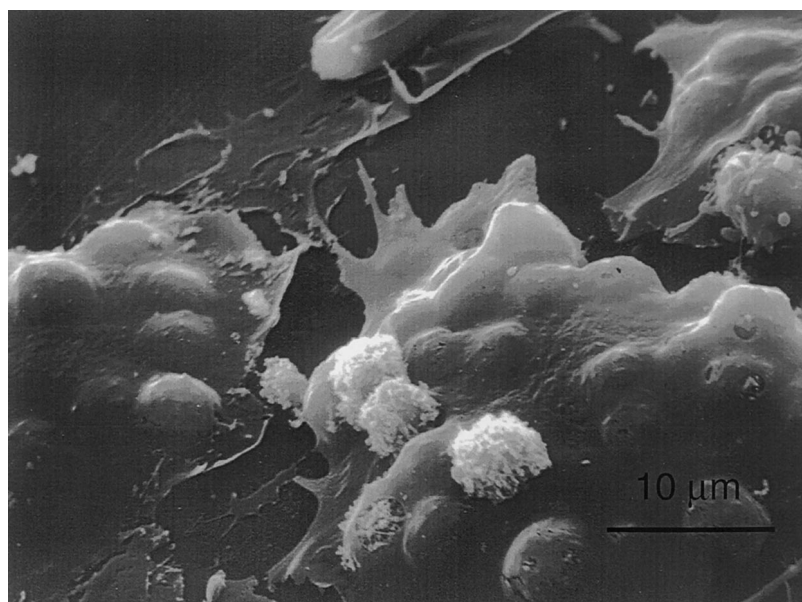


Fig. 1. Schematic of the magnetic twisting stimulator. The dishes containing the cells were put inside the magnetizing and twisting coils, and they were all placed inside an incubator. The coils were cooled with a rubber tubing that delivered circulating water with controlled temperature. The controller, the current source, the defibrillator, and the temperature control were placed outside the incubator for easy manipulation without disturbing the cell dishes. The magnetizing pulse field and the amplitude, duration, and waveform of the applied stress were programmed and automatically applied during the entire experiment.

Fig. 2. A scanning electron micrograph of human umbilical vein endothelial cells (HUVECs) after Arg-Gly-Asp (RGD)-coated beads were bound for >1 h. Most of the beads were internalized, and each cell on average internalized 7–12 beads.



vealed by scanning electron microscopy (Fig. 2). In the absence of the twisting field, the RGD-coated beads that were bound to integrin receptors induced downregulation of ET-1 mRNA expression as the beads were being phagocytosed (Fig. 3). This decrease in ET-1 mRNA reached the lowest value at 2 h after bead binding and gradually returned to the control level after that. Eight hours or longer after bead addition, the ET-1 mRNA recovered back to the prebead-addi-

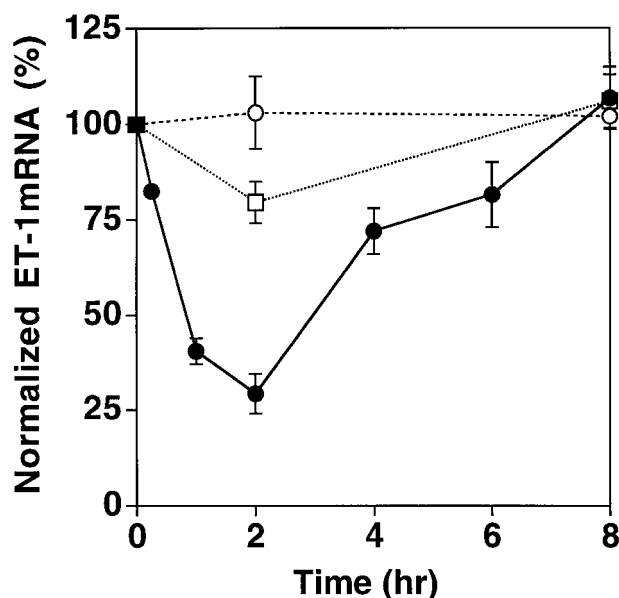


Fig. 3. Time course of endothelin-1 (ET-1) mRNA expression in confluent HUVECs in response to bead binding. ET-1 mRNA expression was normalized to the housekeeping gene glyceraldehyde-3-phosphate dehydrogenase (GAPDH). ●, RGD-coated beads bound to integrin receptors (compared with 0 h,  $P < 0.001$  at 0.25, 1, or 2 h;  $P < 0.01$  at 4 h); ○, acetylated low-density lipoprotein (AcLDL)-coated beads bound to scavenger receptors; □, anti-HLA antibody bound to HLA surface antigen (compared with 0 h,  $P < 0.01$  at 2 h). Means  $\pm$  SE,  $n = 3$  independent experiments.

tion level. These RGD-coated beads were still connected to the actin CSK 8 h after binding when visualized by immunofluorescent confocal microscopy (Fig. 4). In contrast, AcLDL-coated beads that bind to scavenger receptors or anti-HLA antibody-coated beads that bind to HLA class I molecules did not elicit much change in ET-1 mRNA (Fig. 3). Endothelial cells express abundant scavenger receptors and HLA class I molecules on their surface (10, 44).

To investigate whether twisting these beads would induce any changes in ET-1 gene expression, a 20-dyn/cm<sup>2</sup> stress was applied for 2 h after the beads were added to the cells for 6 h. ET-1 mRNA expression was increased by >100% ( $P < 0.005$ ) when the twisting stress was applied to the integrin receptors with RGD-coated beads (Figs. 5 and 6). In contrast, twisting scavenger receptors with AcLDL-coated beads or HLA antigen with anti-HLA antibody-coated beads showed little change in ET-1 mRNA expression. In the absence of the twisting force, binding of RGD-coated beads, but not AcLDL-coated beads or anti-HLA antibody-coated beads, for 8 h, induced slight increases in ET-1 gene expression.

To further explore whether the increase in ET-1 expression was uniform in all cells or only in a subset of cells that was directly stressed, we performed in situ hybridization in the cells. We found that ET-1 mRNA increased only in the cells that were directly stressed using the RGD-coated beads, whereas nearby cells that were not directly stressed did not show upregulation of ET-1 (Fig. 7). No specific signal could be observed using the sense ET-1 probe (not shown).

To investigate the role of stretch-activated (SA) ion channels in twist-induced ET-1 gene expression, HUVECs were treated with gadolinium (20  $\mu$ M) for 30 min before external stress was applied via integrin receptors. Blocking SA channels with gadolinium inhibited stress-induced increases in ET-1 mRNA ex-

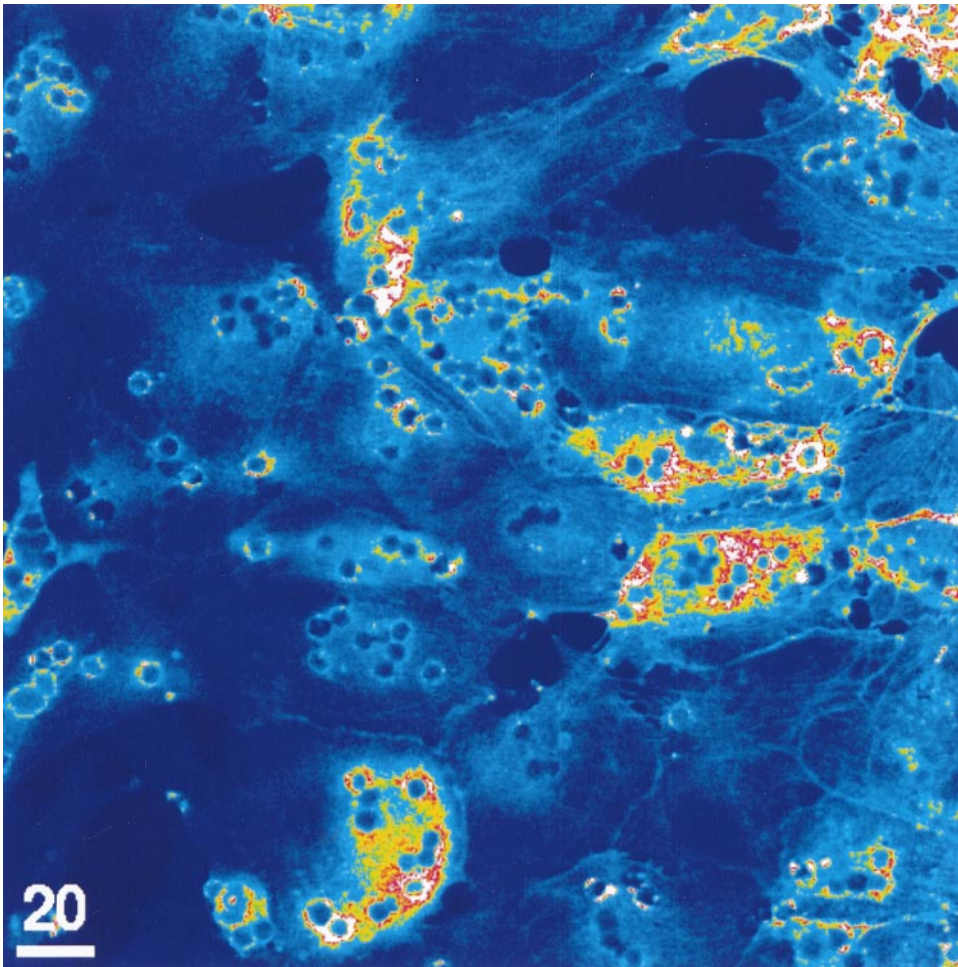


Fig. 4. Immunofluorescent staining of filamentous actin. After RGD-coated beads were bound to HUVECs for 8 h, the cells were fixed and stained with rhodamine-phalloidin. Note that strong fluorescent signals surrounding most of the beads indicate recruitment of filamentous actin to the beads. Scale bar = 20  $\mu$ m.

pression by 65% ( $P < 0.025$ ), although gadolinium alone did not have any inhibitory effects on endogenous expression of ET-1 (Fig. 8). Removal of extracellular  $Ca^{2+}$  with 5 mM EGTA also completely inhibited stress-induced increases in ET-1 gene expression (Fig. 8).

To examine whether protein tyrosine phosphorylation was involved in stress-induced ET-1 expression, cells were pretreated with genistein (20  $\mu$ g/ml) for 2 h before stress application. Genistein alone had no effects on endogenous ET-1 gene expression, whereas

genistein treatment increased ET-1 gene expression in the presence of RGD-coated beads by 50%. However, there was no further increase in ET-1 gene expression in genistein-treated cells in response to applied stress via integrin receptors (Fig. 8).

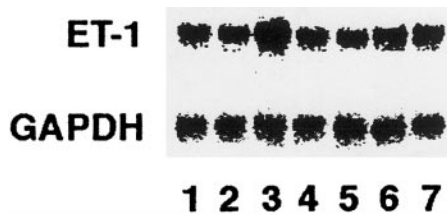


Fig. 5. Northern blot of ET-1 assayed from confluent HUVECs. Lane 1: control; lane 2: RGD-coated beads bound for 8 h; lane 3: twisting RGD-coated beads continuously for 2 h (20 dyn/cm<sup>2</sup>) after the beads were bound for 6 h; lane 4: AcLDL-coated beads bound for 8 h; lane 5: twisting AcLDL-coated beads continuously for 2 h after the beads were bound for 6 h; lane 6: anti-HLA antibody (abHLA)-coated beads bound for 8 h; lane 7: twisting abHLA-coated beads continuously for 2 h after the beads were bound for 6 h. GAPDH: housekeeping gene.

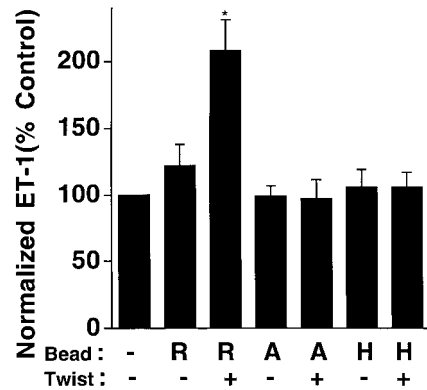
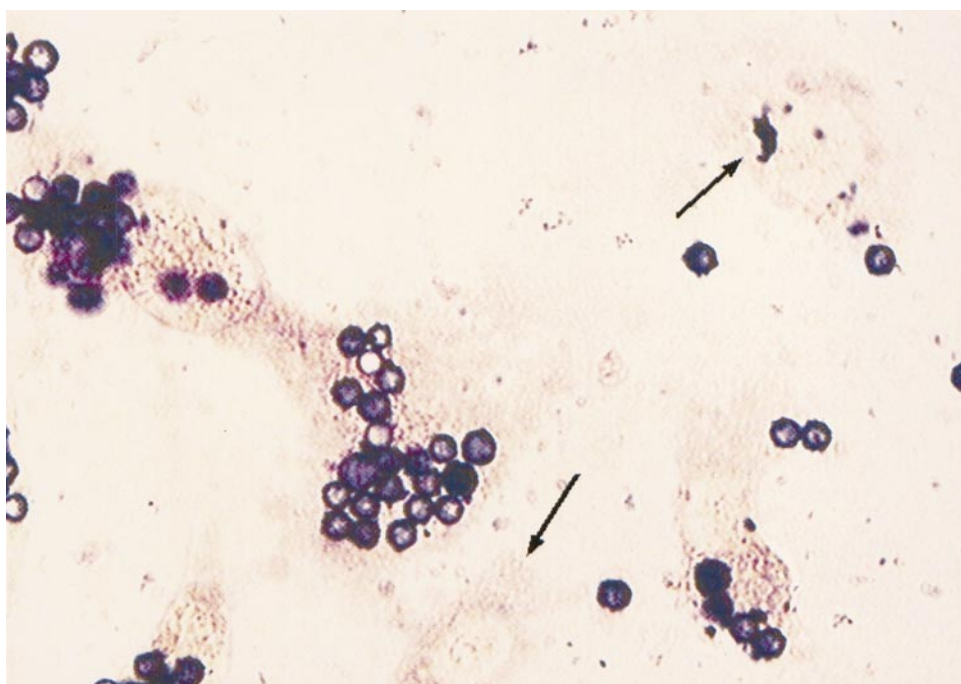


Fig. 6. Normalized ET-1 mRNA expression during different experimental conditions. Bead: -, in the absence of beads; Twist: -, in the absence of twist; +, in the presence of 20 dyn/cm<sup>2</sup> twist for 2 h. R, in the presence of RGD-coated beads,  $n = 6$  independent experiments. A, in the presence of AcLDL-coated beads,  $n = 3$  independent experiments. H, in the presence of abHLA-coated beads,  $n = 3$  independent experiments. Means  $\pm$  SE. Compared with control, it is only statistically significant for RGD-coated beads in the presence of twisting ( $*P < 0.005$ ).

Fig. 7. In situ hybridization of ET-1 mRNA in HUVECs. The cells were twisted with 20 dyn/cm<sup>2</sup> stress for 2 h using RGD-coated beads. The brownish color represents ET-1 mRNA stained by 2-(4-iodophenyl)-5-(4-nitrophenyl)-3-phenyltetrazolium chloride/5-bromo-4-chloro-3-indolyl phosphate-*p*-toluidine salt (INT/BCIP). The arrows point to the neighboring cells that express endogenous ET-1 mRNA.



To test the idea that prestress was important in regulating ET-1 gene expression, an inhibitor of the myosin ATPase, 2,3-butanedione monoxime (BDM), which interferes with actomyosin-based cytoskeletal tension generation (17), was added to the cells in the absence and presence of the twisting force. Treatment with BDM (1 mM) resulted in a small decrease in endogenous ET-1 gene expression. Treatment with BDM in the presence of RGD-coated beads resulted in an additional decrease in ET-1 expression in the ab-

sence of twisting force. Twisting integrin receptors in cells pretreated with BDM 1 h before stress application led to a 65% inhibition in ET-1 mRNA expression compared with control (Fig. 9). Raising BDM concentration to 20 mM completely inhibited endogenous ET-1 gene expression (not shown). Furthermore, treating the cells with a myosin light chain kinase inhibitor, 1-(5-iodonaphthalene-1-sulfonyl)-1*H*-hexahydro-1,4-diazepine HCl (ML-7; 100  $\mu$ M), completely inhibited twist-induced elevation in ET-1 gene expression, al-

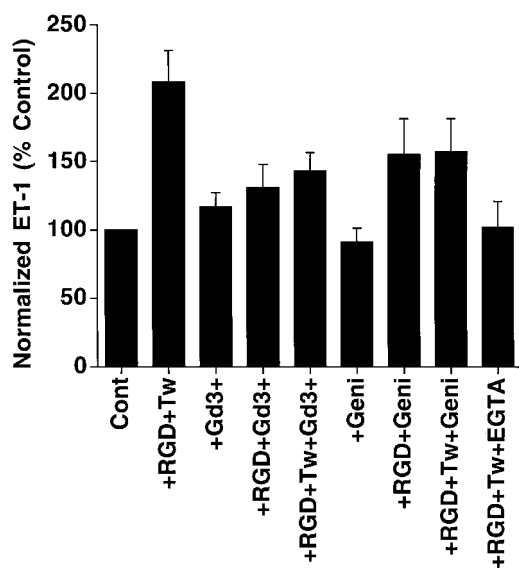


Fig. 8. Normalized ET-1 mRNA expression as a result of twisting and drug treatment. Cont, control; +RGD, RGD-coated beads; +Tw, twisted for 2 h; +Gd<sup>3+</sup>, pretreated with gadolinium for 30 min; +Geni, pretreated with genistein for 2 h; +EGTA, in presence of EGTA. Data are means  $\pm$  SE;  $n = 6$  for Gd<sup>3+</sup>,  $n = 4$  for Geni, and  $n = 3$  for EGTA.  $P < 0.025$  for cells pretreated with Gd<sup>3+</sup> in presence of twist.

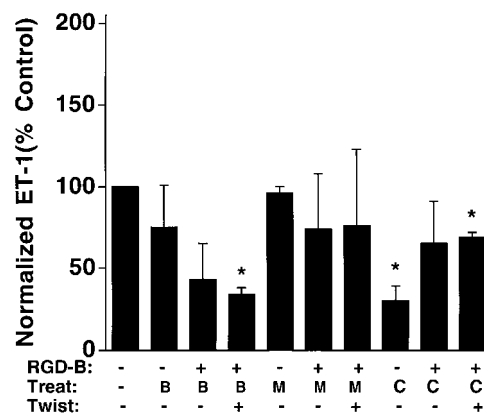


Fig. 9. Normalized ET-1 mRNA expression after different twisting and drug treatments. RGD-B: - represents in the absence of, and + represents in the presence of 20 dyn/cm<sup>2</sup> stress for 2 h. Treat: pretreated with B (2,3-butanedione monoxime or BDM; 1 mM BDM for 1 h to inhibit myosin ATPase); M, 100  $\mu$ M 1-(5-iodonaphthalene-1-sulfonyl)-1*H*-hexahydro-1,4-diazepine HCl) for 10 min to inhibit myosin light chain kinase; C, 0.1  $\mu$ g/ml cytochalasin D for 30 min to disrupt actin cytoskeleton (CSK). Compared with control (lane 1, left), \* $P < 0.01$  for cells pretreated with BDM in the presence of twist; \* $P < 0.01$  for cells treated with cytochalasin D alone; \* $P < 0.005$  for cells pretreated with cytochalasin D in the presence of twist. Means  $\pm$  SE;  $n = 3$  independent experiments for each drug.

though ML-7 alone had no significant effects on ET-1 gene expression. Addition of an actin filament disrupter, Cyto D (0.1  $\mu\text{g}/\text{ml}$  for 30 min), also inhibited stress-induced ET-1 gene expression ( $P < 0.05$ ; Fig. 9). The addition of Cyto D disrupted the integrity of the actin CSK network (Fig. 10). Cyto D alone decreased endogenous ET-1 expression dramatically, as previously observed ( $P < 0.05$ ) (26, 27).

## DISCUSSION

Our results reveal that twisting integrin receptors induced ET-1 gene expression. In contrast, applying stresses to nonadhesion receptors, such as scavenger receptors or HLA antigens, did not elicit changes in ET-1 gene expression. Because scavenger receptors and HLA antigen are both transmembrane receptors that connect only to the membrane cortex and do not associate with cytoplasmic CSK lattice (54), these data demonstrate that membrane deformation alone is not sufficient to induce ET-1 gene expression.

Compared with other existing techniques for applying mechanical stresses, MTS has several advantages: 1) it has no moving mechanical parts; and 2) mechanical stresses can be applied at almost any force pattern, duration, and frequency. Compared with MTC, MTS does not have the capability to quantify mechanical properties. In addition, because the MTS is not shielded, ambient noises such as the Earth's magnetic field might interfere with the applied magnetic field. However, because the Earth's field is only about 0.5 gauss in magnitude, it generates only  $\sim 0.25 \text{ dyn}/\text{cm}^2$  in the absence of a twisting field, much smaller than the applied twisting stress (20  $\text{dyn}/\text{cm}^2$ ). Another potential complication of the method is the inhomogeneity of the attachment of beads to the cells. Completely internalized beads distribute their torque over a larger area than attached but only partially internalized beads. There is an inverse relationship between the contact area and the shear stress exerted on the cell for a given applied torque. Partially internalized beads may produce not only a shear stress, but also a normal stress.

However, we believe that this problem is minimal, in our case, because the beads have attached to the cells for 6 h before the twisting field is turned on. By this time, most beads have been completely internalized, as revealed by scanning electron microscopy (Fig. 2).

Interestingly, beads that are endocytosed via the integrin pathway induced time-dependent downregulation of ET-1 gene expression that reached its maximum effects 2 h after bead binding. Currently, we do not know the underlying mechanisms, but one possibility might be related to endocytosis-induced actin CSK structural rearrangements that could trigger an intracellular signaling pathway, leading to downregulation of ET-1 expression. However, the downregulation is limited to RGD-coated beads, and to a lesser degree, to anti-HLA antibody-coated beads. It is possible that some of the differences in ET-1 gene expression for different ligands might be a result of different degrees of endocytosis. These beads also bind avidly to the cell membrane. Hence, when these beads are twisted by a given applied stress, the cell membrane is deformed much more than when the RGD beads are twisted because these beads rotate more (54). If only the opening of SA channels on the cell membrane and the influx of  $\text{Ca}^{2+}$  were required for ET-1 gene expression, twisting the AcLDL- or anti-HLA antibody-coated beads should have led to higher upregulation of ET-1 gene expression than twisting the RGD beads. Our results are just the opposite. Therefore, it is likely that most of the difference is due to mechanical activation of integrin receptors and deformation of the underlying CSK, which is necessary for the upregulation of ET-1 gene expression.

Inhibition of SA channels has been shown to result in blocking of SA tyrosine phosphorylation (33). Blocking of SA tyrosine phosphorylation, in turn, leads to inhibition of stretch-induced morphological change (33). In this study, we show that inhibition of SA channels with gadolinium blocks twist-induced ET-1 gene expression via integrin receptors, suggesting that SA channels are important in the transduction of mechanical signals into ET-1 gene expression. Furthermore, removal of

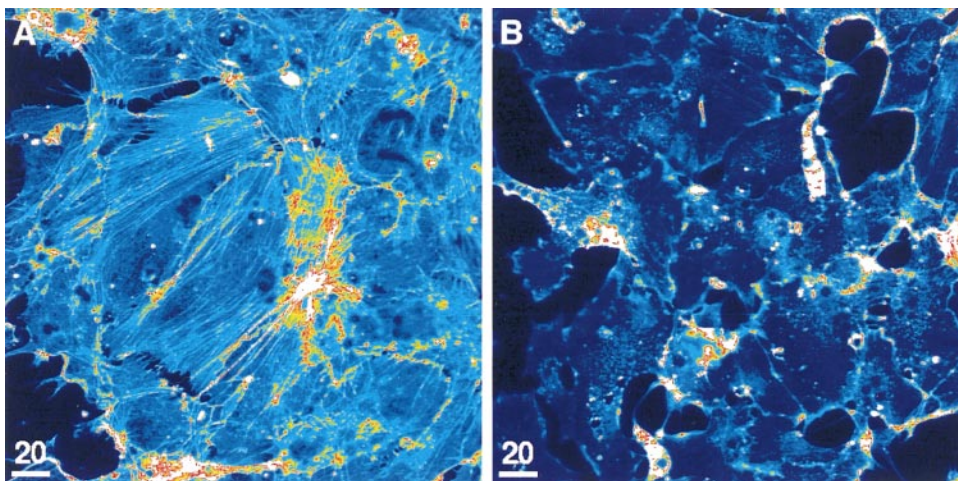


Fig. 10. Rhodamine-phalloidin staining of filamentous actin in HUVECs in the absence (A) and presence (B) of cytochalasin D (0.1  $\mu\text{g}/\text{ml}$  for 30 min). Note that in B, although some RGD-coated beads were still stained with rhodamine-phalloidin, the integrity of the actin CSK was disrupted, and most actin bundles disappeared. Scale bar = 20  $\mu\text{m}$ .

extracellular  $\text{Ca}^{2+}$  with 5 mM EGTA completely inhibited twist-induced ET-1 expression in these cells. A previous study on HUVECs shows that removal of extracellular  $\text{Ca}^{2+}$  does not deplete intracellular  $\text{Ca}^{2+}$  stores (32). Treatment with EGTA or gadolinium does not appear to decrease the affinity or weaken physical interactions between these engulfed RGD-coated beads and the integrin receptors since the resistance from the cells to the rotation of the beads does not decrease (data not shown). Because the beads are in endocytic compartments and isolated from the extracellular medium, how does the mechanical signal reach the plasma membrane where gadolinium and EDTA are presumably acting? There is evidence that SA channels on the membrane are controlled by the underlying CSK (15, 38) that mechanically links the cell membrane with the nucleus (28). The mechanical signals from the beads may reach the plasma membrane via the cytoskeletal network that is physically connected to the endocytic compartments. In other words, these membrane channels can be opened either from outside (e.g., in the case of stretching adherent cells on a flexible membrane) (32) or from inside by deforming the CSK. Together, these results suggest that extracellular  $\text{Ca}^{2+}$  entrance into the cell via the SA channels may be necessary for stress-induced ET-1 gene expression via integrin receptors. However, this interpretation should be taken with caution because factors other than  $\text{Ca}^{2+}$  might also be accountable. In addition, abolishing twist-induced increase in ET-1 expression by inhibiting tyrosine phosphorylation with genistein suggests that tyrosine phosphorylation is part of the mechanotransduction pathway for twist-induced ET-1 gene expression.

Preexisting tension (prestress) in the CSK has been shown to be crucial in regulation of cell shape stability (37) and cell growth (17). Here it is shown that inhibition of CSK prestress with BDM or ML-7 without disrupting the integrity of the CSK completely inhibited twist-induced elevation in ET-1 gene expression. Furthermore, disruption of actin CSK with Cyto D also abolished twist-induced ET-1 gene expression, indicating that the integrity of the actin CSK is crucial in transmitting and transducing mechanical signals into ET-1 gene expression. Although BDM and ML-7 may affect other intracellular processes, our finding indicates that prestress is important in regulating stress-induced ET-1 gene expression.

A previous study shows that ET-1 mRNA expression more than doubles when HUVECs are stretched with 20% strain for 2 h (47), somewhat higher but similar to what we found in our current study. However, because the bead distribution is not likely to be uniform in all cells, the average increase of 100% in ET-1 possibly results from >100% increase in a subpopulation of the cells. Support for this interpretation comes from the results of *in situ* hybridization in which only directly stressed cells exhibited upregulation in ET-1 mRNA (Fig. 7). In addition, the modes of mechanical perturbation are very different. In our study, mechanical rotational stresses were applied locally to apical inte-

grin receptors via an average of 10 beads/cell, whereas in the stretchable membrane method, large global mechanical deformation was applied to all focal adhesions on the basal surface of the cells. The two similar results may suggest the integrin-CSK pathway as the common mechanotransduction pathway for the stretchable membrane method and the twisting technique. In contrast, high levels of fluid flow stress applied for several hours lead to downregulation of ET-1 gene expression (24, 27).

Our current working hypothesis on stress-induced gene expression is that mechanical stress applied via integrins leads to deformation of the membrane and the CSK. Deformation of the membrane opens SA channels, resulting in influx of extracellular  $\text{Ca}^{2+}$ . Increases in intracellular  $\text{Ca}^{2+}$  lead to protein tyrosine phosphorylation. Deformation of the CSK changes enzyme activities and opens the nuclear pores. Both  $\text{Ca}^{2+}$  influx and CSK deformation are necessary for activating downstream transcription factors that lead to increases in ET-1 mRNA expression. Prestress regulates this mechanotransduction process by controlling CSK shape stability and geometrical arrangements of the CSK. CSK, in turn, may control the activation of SA channels due to the physical connections between the channels and the CSK (15, 38). This hypothesis does not exclude potential roles played by other molecules, such as G proteins (14) and phosphatidylinositol 3-kinase (19), which are likely to be part of the complex mechanotransduction process. Alternatively, a membrane model (7) states that mechanical force transmission and transduction occur only at the membrane cortex (a thin layer of lipid membrane and the underlying actin cortex, ~50–100 nm), and, subsequently, diffusion-based mechanisms dictate the downstream events in the cytoplasm and the nucleus. However, the present results showing the specificity of phagocytosed ligand-coated beads in twist-induced ET-1 upregulation do not appear to be consistent with the membrane model.

Using the MTC technique, we have previously shown that integrins directly mediate mechanical stresses across the cell surface and into the CSK, whereas nonadhesion molecules, such as AcLDL, do not mediate mechanical force transfer across the cell surface (49). We have also shown that vinculin mechanically couples the integrins with the CSK (12, 13). Mechanical stresses applied via integrins result in coordinated changes in cytoskeletal structure and nuclear shape (28). Furthermore, it has been shown that mechanical stresses applied via integrins lead to increases in intracellular  $\text{Ca}^{2+}$  (35). Tyrosine phosphorylation is altered by stressing magnetic beads bound to integrin receptors using a similar magnetic twisting device or a magnetic pulling device (1, 2, 41). In addition, recruitment of ribosomes and mRNA to the focal adhesion complexes is increased after mechanically twisting the integrin receptor (5). Blocking integrins with antagonists leads to inhibition of fluid shear stress effects on endothelial cells, mechanical strain effects on smooth muscle cells, and substrate deformation on bone cells (31, 39, 53). Interestingly, a recent independent study

shows that mechanical stress applied to integrin receptors via magnetic beads activates the cAMP cascade and downstream gene transcription (29). However, these authors find that an intact CSK is not required for activation of the cAMP cascade. It is possible that some molecules that are associated with the cell membrane can be activated mechanically in the absence of the CSK, whereas more complex cell functions (such as ET-1 gene expression or cell growth) require an intact CSK and active CSK tension to transduce mechanical signals into biological responses.

What is the biological relevance of applying stresses via integrins on the apical surface of the cell? After RGD beads bind to integrin receptors on the apical surface of the cells, focal adhesion complexes (3) are formed surrounding the beads on the apical surface (49). Shear stresses applied via these beads represent a situation that is different from applying fluid shear stress on the apical surface of the cells or stretching adherent cells via extracellular matrix-integrin interactions at the basal surface. However, there is evidence that application of fluid shear stress to the luminal surface of the endothelial cells results in alterations at the abluminal focal adhesion complexes (9). Furthermore, recent results show that extracellular signal-regulated kinase and c-Jun NH<sub>2</sub>-terminal kinase activation by mechanical stretch is integrin dependent (23). Therefore, applying shear stresses via magnetic microbeads to integrin receptors appears to be a physiologically relevant approach that can be used to probe the molecular mechanisms of mechanical signaling. It remains to be elucidated what the signaling pathway of stress-induced ET-1 gene expression via integrin receptors is and whether different amplitudes, patterns, and frequencies of mechanical stresses and different subsets of integrin receptors would result in different responses in these cells.

In summary, we have developed a technique that can apply twisting mechanical stresses to specific receptors with different amplitudes, force patterns, duration, and frequencies. Using this method, we have shown that ET-1 gene expression is upregulated when integrin receptors are twisted. MTS could be useful in studying molecular mechanisms of mechanochemical transduction and biological responses.

We thank Drs. H. Wang, Arthur Lee, Joe Paulauskis, and M. Chicurel for generous gifts of reagents, Marie-France Lavoie for technical assistance, Jean Lai for confocal microscopy, and Drs. Don Ingber and Jeff Fredberg for continued support.

This work was supported by National Heart, Lung, and Blood Institute Grants HL-65371 and HL-33009, National Aeronautics and Space Administration Grant NAG54839 (to N. Wang), and a Deutsche Forschungsgemeinschaft fellowship (to B. Fabry).

## REFERENCES

1. Bierbaum S and Notbohm H. Magnetomechanical stimulation of mesenchymal cells. In: *Scientific and Clinical Applications of Magnetic Carriers*, edited by Hafeli U, Wolfgang D, and Schmit P. New York: Plenum, 1997, p. 311–322.
2. Bierbaum S and Notbohm H. Tyrosine phosphorylation of 40 kDa proteins in osteoblastic cells after mechanical stimulation of  $\beta_1$ -integrins. *Eur J Cell Biol* 77: 60–67, 1998.
3. Burridge K, Fath K, Kelly T, Nuckolls G, and Turner C. Focal adhesions: transmembrane junctions between the extracellular matrix and the cytoskeleton. *Annu Rev Cell Biol* 4: 487–525, 1998.
4. Chicurel ME, Chen CS, and Ingber DE. Cellular control lies in the balance of forces. *Curr Opin Cell Biol* 10: 232–239, 1998.
5. Chicurel ME, Singer RH, Meyer CM, and Ingber DE. Recruitment of mRNA and ribosomes to focal adhesions triggered by integrin binding and mechanical tension. *Nature* 392: 730–733, 1998.
6. Choquet D, Felsenfeld DP, and Sheetz MP. Extracellular matrix rigidity causes strengthening of integrin-cytoskeleton linkages. *Cell* 88: 39–48, 1997.
7. Dai J and Sheetz MP. Regulation of endocytosis, exocytosis, and shape by membrane tension. *Cold Spring Harb Symp Quant Biol* 60: 567–571, 1995.
8. Davies PF. Flow-mediated endothelial mechanotransduction. *Physiol Rev* 75: 519–560, 1995.
9. Davies PF, Robotewskyj A, and Griem MI. Quantitative studies of endothelial cell adhesion: directional remodeling of focal adhesion sites in response to flow forces. *J Clin Invest* 93: 2031–2038, 1994.
10. Epperson DE, Arnold D, Spies T, Cresswell P, Pober JS, and Johnson DR. Cytokines increase transporter in antigen processing-1 expression more rapidly than HLA class I expression in endothelial cells. *J Immunol* 149: 3297–3301, 1992.
11. Evans E and Yeung A. Apparent viscosity and cortical tension of blood granulocytes determined by micropipette aspiration. *Biophys J* 56: 151–160, 1989.
12. Ezzell RM, Goldmann WH, Wang N, Parashama N, and Ingber DE. Vinculin promotes cell spreading by mechanically coupling integrins to the cytoskeleton. *Exp Cell Res* 231: 14–26, 1996.
13. Goldmann WH, Galneder R, Ludwig M, Xu W, Adamson ED, Wang N, and Ezzell RM. Differences in elasticity of vinculin-deficient F9 cells measured by magnetometry and atomic force microscopy. *Exp Cell Res* 239: 235–242, 1998.
14. Gudi S, Nolan JP, and Frangos JA. Modulation of GTPase activity of G proteins by fluid shear stress and phospholipid composition. *Proc Natl Acad Sci USA* 95: 2515–2519, 1998.
15. Hamill OP and McBride DW Jr. The pharmacology of mechanogated membrane ion channels. *Pharmacol Rev* 48: 231–252, 1996.
16. Hochmuth RM. Micropipette suction of living cells. *J Biomech* 33: 15–22, 2000.
17. Huang S, Chen CS, and Ingber DE. Control of cyclin D1, p27Kip1, and cell cycle progression in human capillary endothelial cells by cell shape and cytoskeletal tension. *Mol Biol Cell* 9: 3179–3193, 1998.
18. Hubmayr R, Shore SA, Fredberg JJ, Planus E, Panettieri RA Jr, Moller W, Heyder J, and Wang N. Pharmacological activation changes stiffness of cultured human airway smooth muscle cells. *Am J Physiol Cell Physiol* 271: C1660–C1668, 1996.
19. Hubner S, Couvillon AD, Kas JA, Bankaitis VA, Vegners R, and Janmey PA. Enhancement of phosphoinositide 3-kinase (PI 3-kinase) activity by membrane curvature and inositol-phospholipid-binding peptides. *Eur J Biochem* 258: 846–853, 1998.
20. Ingber DE. Cellular tensegrity; defining new rules of biological design that govern the cytoskeleton. *J Cell Sci* 104: 613–627, 1993.
21. Lee KM, Tsai KY, Wang N, and Ingber DE. Extracellular matrix and pulmonary hypertension: control of vascular smooth muscle cell contractility. *Am J Physiol Heart Circ Physiol* 274: H76–H82, 1998.
22. Levesque MJ and Nerem RM. The study of rheological effects of vascular endothelial cells in culture. *Biorheology* 26: 345–357, 1989.
23. MacKenna DA, Dolfi F, Vuori K, and Ruoslahti E. Extracellular signal-regulated kinase and c-Jun NH<sub>2</sub>-terminal kinase activation by mechanical stretch is integrin-dependent and matrix-specific in rat cardiac fibroblasts. *J Clin Invest* 101: 301–310, 1998.

24. **Malek A and Izumo S.** Physiological fluid shear stress causes downregulation of endothelin-1 mRNA in bovine aortic endothelium. *Am J Physiol Cell Physiol* 263: C389–C396, 1992.
25. **Malek AM, Greene AL, and Izumo S.** Regulation of endothelin 1 gene by fluid shear stress is transcriptionally mediated and independent of protein kinase C and cAMP. *Proc Natl Acad Sci USA* 90: 5999–6003, 1993.
26. **Malek AM, Lee LW, Alper SL, and Izumo S.** Regulation of endothelin-1 gene expression by cell shape and the microfilament network in vascular endothelium. *Am J Physiol Cell Physiol* 273: C1764–C1774, 1997.
27. **Malek AM, Zhang J, Jiang J, Alper SL, and Izumo S.** Endothelin-1 gene suppression by shear stress: pharmacological evaluation of the role of tyrosine kinase, intracellular calcium, cytoskeleton, and mechanosensitive channels. *J Mol Cell Cardiol* 31: 387–399, 1999.
28. **Maniotis AJ, Chen CS, and Ingber DE.** Demonstration of mechanical connection between integrins, cytoskeletal filaments, and nucleoplasm that stabilize nuclear structure. *Proc Natl Acad Sci USA* 94: 849–854, 1997.
29. **Meyer CJ, Alenghat FJ, Rim P, Fong JHJ, Fabry B, and Ingber DE.** Mechanical control of cyclic AMP signaling and gene transcription through integrins. *Nat Cell Biol* 2: 1–3, 2000.
30. **Morita T, Kurihara H, Maemura K, Yoshizumi M, and Yazaki Y.** Disruption of cytoskeletal structures mediates shear stress-induced endothelin-1 gene expression in cultured porcine aortic endothelial cells. *J Clin Invest* 92: 1706–1712, 1993.
31. **Muller JM, Chilian WM, and Davis MJ.** Integrin signaling transduces shear stress-dependent vasodilation of coronary arterioles. *Circ Res* 80: 320–326, 1997.
32. **Naruse K and Sokabe M.** Involvement of stretch-activated ion channels in  $Ca^{2+}$  mobilization to mechanical stretch in endothelial cells. *Am J Physiol Cell Physiol* 264: C1037–C1044, 1993.
33. **Naruse K, Ymada T, and Sokabe M.** Involvement of SA channels in orienting response of cultured endothelial cells to cyclic stretch. *Am J Physiol Heart Circ Physiol* 274: H1532–H1538, 1998.
34. **Peterson NO, McConnaughey WB, and Elson EL.** Dependence of locally measured cellular deformability on position on the cell, temperature, and cytochalasin B. *Proc Natl Acad Sci USA* 79: 5327–5331, 1981.
35. **Pommerenke H, Schreiber E, Durr F, Nebe B, Hahnel C, Moller W, and Rychly J.** Stimulation of integrin receptors using a magnetic drag force device induces an intracellular free calcium response. *Eur J Cell Biol* 70: 157–164, 1996.
36. **Potard USB, Butler JP, and Wang N.** Cytoskeletal mechanics in confluent epithelial cells probed through integrins and E-cadherins. *Am J Physiol Cell Physiol* 272: C1654–C1663, 1997.
37. **Pourati J, Maniotis A, Spiegel D, Schaffer JL, Butler JP, Fredberg JJ, Ingber DE, Stamenovic D, and Wang N.** Is cytoskeletal tension a major determinant of cell deformability in adherent endothelial cells? *Am J Physiol Cell Physiol* 274: C1283–C1289, 1998.
38. **Sachs F.** Mechanical transduction in biological systems. *Crit Rev Biomed Eng* 16: 141–169, 1988.
39. **Salter DM, Robb JE, and Wright MO.** Electrophysiological responses of human bone cells to mechanical stimulation: evidence for specific integrin function in mechanotransduction. *J Bone Miner Res* 12: 1133–1141, 1997.
40. **Schiffrin EL, Deng LY, Sventek P, and Day R.** Enhanced expression of endothelin-1 gene in resistance arteries in severe human essential hypertension. *J Hypertens* 15: 57–63, 1997.
41. **Schmidt C, Pommerenke H, Durr F, Nebe B, and Rychly J.** Mechanical stressing of integrin receptors induces enhanced tyrosine phosphorylation of cytoskeletally anchored proteins. *J Biol Chem* 273: 5081–5085, 1998.
42. **Sharffkin JB, Diamond SL, Eskin SG, McIntire LV, and Dieffenbach CW.** Fluid flow decreases preproendothelin mRNA levels and suppresses endothelin-1 peptide release in cultured human endothelial cells. *J Vasc Surg* 14: 1–9, 1991.
43. **Shroff SG, Saner DR, and Lal R.** Dynamic micromechanical properties of cultured rat arterial myocytes measured by atomic force microscopy. *Am J Physiol Cell Physiol* 269: C286–C292, 1995.
44. **Sprague EA, Kothapalli R, Kerbacher JJ, Edwards EH, Schwartz CJ, and Elbein AD.** Inhibition of scavenger receptor-mediated modified low-density lipoprotein endocytosis in cultured bovine aortic endothelial cells by the glycoprotein processing inhibitor castanospermine. *Biochemistry* 32: 8888–8895, 1993.
45. **Sumpio BE and Banes AJ.** Response of porcine aortic smooth muscle cells to cyclic tensional deformation in culture. *J Surg Res* 44: 696–701, 1993.
46. **Tagawa H, Wang N, Narishige T, Ingber DE, Zile MR, and Cooper G IV.** Cytoskeletal mechanics in pressure-overload cardiac hypertrophy. *Circ Res* 80: 281–289, 1997.
47. **Wang DL, Tang CC, Wung BS, Chen HH, Hung MS, and Wang JJ.** Cyclical strain increases endothelin-1 secretion and gene expression in human endothelial cells. *Biochem Biophys Res Commun* 195: 1050–1056, 1993.
48. **Wang N.** Mechanical interactions among cytoskeletal filaments. *Hypertension* 32: 162–165, 1998.
49. **Wang N, Butler JP, and Ingber DE.** Mechanotransduction across the cell surface and through the cytoskeleton. *Science* 260: 1124–1127, 1993.
50. **Wang N and Ingber DE.** Control of cytoskeletal stiffness by extracellular matrix, cell shape, and mechanical tension. *Biophys J* 66: 1281–1289, 1994.
51. **Wang N and Ingber DE.** Probing transmembrane mechanical coupling and cytomechanics using magnetic twisting cytometry. *Biochem Cell Biol* 73: 327–335, 1995.
52. **Wang N, Plannus E, Pouchelet M, Fredberg JJ, and Barlovatz-Meimom G.** Urokinase receptor mediates mechanical force transfer across the cell surface. *Am J Physiol Cell Physiol* 268: C1062–C1066, 1995.
53. **Wilson E, Sudhir K, and Ives HE.** Mechanical strain of rat vascular smooth muscle cells is sensed by specific extracellular matrix/integrin interactions. *J Clin Invest* 96: 2364–2372, 1995.
54. **Yoshida M, Westlin WF, Wang N, Ingber DE, Rosenzweig A, Resnick N, and Gimbrone MA Jr.** Leukocyte adhesion to vascular endothelium induces E-selectin linkage to the actin cytoskeleton. *J Cell Biol* 133: 445–455, 1996.
55. **Yoshizumi M, Kurihara H, Sugiyama T, Takaku F, Yanagisawa M, Masaki T, and Yazaki Y.** Hemodynamic shear stress stimulates endothelin production by cultured endothelial cells. *Biochem Biophys Res Commun* 161: 859–864, 1989.